Journal of Veterinary Internal Medicine
Open Access

Standard Article

J Vet Intern Med 2017;31:854–863

Validation of a Multiplexed Gene Signature Assay for Diagnosis of Canine Cancers from Formalin-Fixed Paraffin-Embedded Tissues

B. Davis, M. Schwartz, D. Duchemin, J. Carl Barrett, and G. Post

Background: Use of molecular-based diagnostics for companion animals is impeded by availability of technology platforms, tissue acquisition requirements, and species-specific reagents.

Hypothesis/Objectives: To validate a quantitative nuclease protection assay (qNPA) to simultaneously measure RNA expression of multiple genes in archived formalin-fixed paraffin-embedded (FFPE) tumors from dogs.

Animals: All tumor biopsy samples were collected retrospectively from surgical biopsies and in the care of veterinarians.

Methods: Retrospective case series. A qNPA 96-well ArrayPlate was built using 30 canine-specific genes, 5 housekeeping genes, positive and negative controls with qualified gene-specific oligonucleotides. Pearson's correlation, coefficient of variation (CV), and multivariate analysis were used to determine analytical performance using 40 FFPE dog tumors. Once validated, 70 FFPE dog tumors were analyzed for differences in gene expression using hierarchical clustering and analysis of variance of log transformed data. Immunohistochemistry (IHC) was performed to correlate gene expression and protein expression in a subset of tumors.

Results: The assay was linear with decreasing sample input (R^2 = 0.978), reproducible within and between 96-well plates (r = 0.988 and 0.95, respectively) and between different laboratories (CV = 0.96). Hierarchical cluster analysis showed grouping of tumors by histogenesis and oncogenes. Significant differences were found between BCl2, E2F transcription factor 1, MDM2, COX-2, MET proto-oncogene receptor kinase, and other biologically relevant gene expression in tumor subtypes. Immunohistochemistry confirmed protein expression.

Conclusions and Clinical Implications: Because this technology works reliably on FFPE specimens, it can help expedite the broad introduction of multiplexed genomic information for improved diagnostics and discovery of new targets for therapies in veterinary oncology.

Key words: Algorithms; Dog; Genomics; Lymphoma; RNA; Sarcoma.

Use of genomic information has greatly advanced the care of people with cancer and can serve as a roadmap for the future of veterinary oncology. Thus far, limited molecular studies in companion animals have demonstrated the utility of examining gene signatures of tumors to discover potential biomarkers of outcome and treatment.[1–5] However, in clinical veterinary practice use of genomic information for supportive diagnostics remains unfulfilled. A complimentary approach using gene expression profiling is highly useful in studies of human cancers and can be extrapolated to cancers in dogs. In diagnosing canine cancers, formalin fixation is the standard tissue collection method in daily clinical practice, but formalin fixation remains a major obstacle in analyzing gene expression. For most gene expression profiling technologies, fresh or frozen samples are recommended because formalin fixation causes cross-linking of RNA (and protein), nucleic acid fragmentation, and the addition of monomethylol groups to

Abbreviations:

ABCB1	ATP-binding cassette, sub-ABCB1family B (MDR/TAP), member 1
Bcl2	B-cell lymphoma 2 (Bcl-2)
BRCA1	breast cancer related gene 1
CDH1	E-cadherin
COO	cell of origin
CV	coefficient of variation
DES	desmin
DLBCL	diffuse large B-cell Lymphomas
DLs	detection linkers
E2F1	E2F transcription factor 1
EGFR	epidermal growth factor receptor
ERBB2	Erb-B2 receptor tyrosine kinase 2
ERCC1	excision repair cross-complementation group 1
ESR1	estrogen receptor
FFPE	formalin-fixed paraffin-embedded
H&E	hematoxylin and eosin
IHC	immunohistochemistry
iUC	invasive urethelial cancer
MDM2	mouse double minute 2 homologue
MET	MET proto-oncogene receptor kinase
MGMT-O-6	methylguanine DNA methyltransferase
Mitogen	activated protein kinase kinase 1-MAP2K1
Mitogen	activated protein kinase kinase 2- MAP2K2
MLNA	melanin A
Myc	MYC proto-oncogene
NPPs	nuclease protection probes
PLs	program linkers
PR	progesterone receptor
PTGS-2	prostaglandin synthase-2
qNPA	quantitative nuclease protection
STS	soft tissue sarcoma
TCC	transitional cell carcinomas
TYRP1	tyrosinase-related protein 1
VIM	vimentin

From Innogenics Inc, Harvard, MA (Davis, Duchemin, Barrett, Post); HTG Molecular Inc, Tucson, AZ (Schwartz); and the Veterinary Cancer Center, Norwalk, CT (Duchemin, Post).

Corresponding author: B. Davis, Innogenics Inc, Harvard, MA; e-mail: BDavis@innogenics.com.

Submitted May 31, 2016; Revised January 5, 2017; Accepted February 7, 2017.

DOI: 10.1111/jvim.14686

the bases, which introduces artifacts and interferes with reverse transcription and amplification processes used for PCR-based gene expression and sequencing studies. PCR-based molecular studies can be performed on formalin-fixed paraffin-embedded (FFPE) tissues, but the RNA integrity must be carefully evaluated and archived samples often have small fragments that prove particularly difficult to analyze. To overcome the challenges of formalin fixation for genomic-based studies, a quantitative nuclease protection assay (qNPA) was developed that reliably analyzes small and fragmented mRNA expression in small samples of FFPE tissues.[6,7]

The key to qNPA methodology is the capability of measuring mRNA species without steps of mRNA extraction, cDNA synthesis, or gene amplification.[6,8] Briefly, qNPA involves hybridization of 50-mer probes to form a proportional 1 : 1 probe-to-specific mRNA concentration of interest and after nuclease digestion uses fluorescent probes to quantitatively measure levels of mRNA based on emitted light. The reproducibility, repeatability, and applicability of this assay is well established in studies using human samples.[6,7,9] Utility of qNPA for gene expression was first validated using fresh, frozen, and FFPE samples from people with diffuse large B-cell lymphomas (DLBCL), and a prognostic qNPA array panel was subsequently developed using paraffin blocks of tissue previously frozen and analyzed by microarray gene expression.[10] Validation steps showed assay linearity, specificity for mRNA measurement, and an excellent correlation ($R^2 > 0.98$) between fresh, frozen, and FFPE samples.[6] Gene expression was confirmed by immunohistochemistry (IHC) for 3 genes, and qNPA was further correlated to genes from an Affymetrix-based microarray gene expression study. Newly prepared FFPE blocks were compared to archived blocks >20 years old ($R^2 > 0.70$). As studies demonstrated the therapeutic impact of classifying DLBCL based on its cell of origin (COO) molecular subtype rather than histology, a COO-based qNPA array also proved reliable and practical for FFPE samples of DLBCL.[11] The COO gene expression array was deemed superior over IHC-based algorithms for COO determination due to the subjective qualitative interpretation of IHC results and marked intra-observer and interlaboratory variations.[11]

Given the proven analytical and clinical validity of qNPA-based assays using FFPE biopsy samples in human oncology, we sought to translate this methodology to veterinary oncology using diagnostic biomarkers with the potential to guide therapy. This study details the requirements needed to validate a test—analytical precision, reliability and reproducibility and clinical validity or "fit for purpose."[12,13]

Materials and Methods

Quantitative Nuclease Protection Assay Specifics

Three oligonucleotides are required to quantify a targeted mRNA sequence: a nuclease protection probe, a programming linker, and a detection linker (DL) (Fig S1). The nuclease protection probes (NPPs) are hybridized to all target RNA, both soluble and cross-linked. S1 nuclease is then added as a single strand cleanup step, destroying nonspecific RNA and excess NPPs. This reaction produces a stoichiometric amount of target RNA/NPP duplexes. Base hydrolysis of the RNA releases the NPPs from the duplexes. A mixture of custom programming linkers (PLs) is then added with each PL capturing a gene-specific NPP. DLs, of which half of the DL is complementary to its corresponding NPP, are hybridized to the samples followed by addition of a biotinylated detection probe. This hybridizes to the generic portion of the DL. The detection enzyme (Avidin-HRP conjugate) is added, which hybridizes to the biotin moiety on the detection probes, and the sample mRNA is then quantitated via light detection and image analysis software (HTG Molecular, Tucson, AZ). The qNPA platform is in a 96-well format, with each well capable of evaluating up to 43 different genes, including a universal RNA positive control and a plant RNA negative control.

Canine Array Build

For the canine array, 30 canine genes were selected a priori for the array based on their diagnostic utility or known drug target and responses either in the veterinary or human literature. Canine-specific gene sequences were identified using the third build of the Canine Genome in the National Center for Biotechnology Information (NCBI). RefSeq Database was used as the reference genome for comparison purposes. The targeted gene sequences were obtained from a combination of RefSeq and ENSEMBL databases. Table S1 lists these genes and the Omnibus Accession Number. The gene sequences were monitored to ensure the absence of potential secondary structure and were subjected to BLAST-like searches against other reported canine sequences to ensure significant homology or complementarity with other genes did not exist in the array. The oligonucleotide probes for the canine-specific gene array were developed through a series of testing and validation studies. These included oligonucleotide QC, array assembly, and implementation on an automated HTG Edge System[a] . The programming linkers and NPPs were ordered in an HPLC purified format. All oligonucleotides were then tested experimentally before their use in the finalized array analysis. This analysis was performed to ensure that each oligonucleotide hybridized as expected without showing unintended binding, which would interfere with the array assembly. DNA oligonucleotides were quality checked to ensure that each oligonucleotide functioned as intended by separating each target set for PLs, NPPs, and DLs and then were added to an ArrayPlate (Fig S2). Any probe sets failing to meet QC criteria were resynthesized before proceeding to the array assembly step.

A universal 96-well ArrayPlate was built using the previously identified and qualified gene-specific oligonucleotides. Array analysis and implementation were performed over a series of experiments using 45 tumors of commonly encountered tumors in dogs including sarcomas (osteosarcomas, hemangiosarcomas, soft tissue sarcomas), carcinomas (thyroid, anal sac, transitional cell, mammary gland), B-cell and T-cell lymphomas, and melanomas. In a preliminary sampling of tissues, qNPA identified RNA in all samples except osteosarcomas and subungual melanomas. The lack of RNA from the later tissues was attributed to the rapid acid-based decalcification process, and these tumors were excluded from further analysis. Subsequently, array development was based on a titration using 4 carcinoma, 4 sarcoma, 4 oral melanomas, and 3 lymphoma tumor samples to determine (1) the linear response of the genes to varying amounts of sample input; (2) reproducibility of the array as expressed through coefficient of variation (CV) across a technical replicate; and (3) confirmation of the optimal sample input amount for each tissue and sample type. Final

implementation of the array was performed on a total of 30 FFPE canine tumor samples and reagents optimized with the initial sample cohort at the previously determined optimal sample amount for each sample type. Human universal RNA was also analyzed in triplicate at 100 ng/well on each plate as a qNPA run control. Forty-five potential housekeeping genes (HK genes or endogenous controls) were selected based on previous experience or prevalence in the literature and evaluated against 15 canine tumor and normal tissue samples (Table S2). Samples were analyzed in triplicate and assessed for data quality based on averaged signals, standard deviations, and technical (intrareplicate) CV.

Samples

Tumor biopsy samples were collected retrospectively from surgical biopsies of companion dogs performed for diagnostic purposes and for which original pathology reports were available. Tumor classifications including grade of soft tissue sarcomas were based on original and independent histopathological reports accompanying samples. Because these samples were routinely collected in a clinical situation, time from sample collection to formalin fixation was not documented, but clinical experience is that biopsy samples are fixed within a window of time that allows for adequate preservation. The samples used in these studies were archived for 2 years or less. All animal care was taken in accordance with standard practices and in the care of veterinarians. No live animals were used in these studies.

For qNPA studies, biopsies were rereviewed on hematoxylin and eosin (H&E) stained slides and cancerous areas were identified. The H&E stained slide was placed over each of at most 5 sections of 5 μm unstained serial sections for macrodissection of tumor. Optimal amount of tissue from the FFPE unstained slides was scraped into microcentrifuge tubes to which proprietary lysis buffer[a] was added and overlaid with 500 μL of mineral oil. The samples were heated for 15 minutes at 95°C to melt paraffin. Proteinase K was added and samples then mixed and incubated at 50°C for 1 hour. Samples were then pipetted in triplicate into a 96-well sample plate. The sample plate was then transferred to the HTG Edge Processor. The HTG Edge Processor automated all the chemistry from post sample preparation up to transferring completed qNPA reactions into the ArrayPlate over a 27-hour time period. Imaging, reading and data capture was performed with the HTG Reader that automated all reading processes from addition of the chemiluminescent substrate in each well to imaging and data capture over a 30-minute time period.

For IHC studies, tumor samples were selected for staining based on results of the qNPA analysis and for which corresponding sections were available for staining. Antibodies were selected from commercial sources that were documented to work in FFPE, was of size and specificity for the protein of interest by Western blot or reported cross-reactivity to dog protein (Table S3). Additionally, all antibodies were tested in-house on dog tissues using dilutions and positive and negative controls. All slides were deparaffinized and hydrated to deionized (DI) water. Antigen retrieval methods were citrate[b] for 20 minutes in a steamer for all antibodies except MET proto-oncogene receptor kinase (MET), which was retrieved using EDTA[c] for 20 minutes in steamer. Slides were cooled for 15 minutes and rinsed twice in DI water. Endogenous peroxides were blocked in 3% hydrogen peroxide 2 times for 5 minutes each, and then, slides rinsed twice in DI water. Primary antibody was added at the designated concentration for 30 minutes after a 20 minute casein protein block. Slides were rinsed in phosphate-buffered saline. Hi-Def Polymer[b] as per manufacturer was used for antibody detection except for MET for which Mach 2 anti-rb polymer (Biocare) was used. Slides were stained with DAB and counterstained with hematoxylin for visualization. Controls were of appropriate tissues with depletion of primary antibody and corresponding serum control. Staining intensity was assessed using H-score that accounts for staining intensity on a scale of 1–3 and the percentage of cells that are stained according to the formula: [1 × % cells 1+) + 2 × (% cell 2+) + 3 × (% cells 3+)].

Statistics

Analytical evaluation of assay performance was carried out by Pearson's correlation to determine CV and multivariate analysis. Captured images were analyzed by the HTG Edge System Software and HTG Molecular imaging algorithms. Output was a Microsoft Excel spreadsheet format which detailed raw image intensity values from all wells in triplicate. Values were filtered (not reported) for wells in which the positive control was not detected above a predetermined cutoff. Values were then normalized to intensity levels of the 5 HK genes according to the formula: (Signal of value × (#Housekeeping genes))/Sum (Signals of all housekeeping genes). Triplicate values were averaged and reported with S.D. and CV. If CV was >22%, values were discarded. Diagnostic algorithms were developed and applied to identify gene expression levels at least 2-fold over background intensity levels. Hierarchical analysis and nonparametric analysis of gene expression within and across tumor types and grades using Wilcoxon/al–Wallis Tests (Rank Sums) and least squares analysis were performed with JMP, Version *13* statistical software package[d] . The logarithms of gene expression values were used to standardize the data for statistical comparisons. The significance threshold was set at 0.05.

Results

Technical Validity

Selected HK genes showed abundant expression level with relatively low (2- to 3-fold) intensity levels across all tumors. To test linearity of the assay and to determine the optimal tissue amount for the final array, a 7-point serial dilution was performed for tumor types beginning with a concentration of 0.4 cm^2/well for each tumor type. Table S4 shows a representative data set for a lymphoma sample from the multipoint titration. The average linearity of all titrated samples was $R^2 = 0.978$. Optimal sample size was determined to be 0.2, 0.4, 0.2, and 0.2 cm^2/well for carcinomas, sarcomas, melanomas, and lymphomas, respectively.

For array implementation, 30 tumor samples were split across 3 plates, with 2 plates being processed on the same HTG Edge System, and the third plate run on a separate HTG Edge System at the recommended concentration for each sample. The average Pearson's correlation coefficient was $r = 0.988$ for all samples when run on the same HTG Edge System, and 0.985 when run on separate HTG Edge Systems. The CVs comparing between each of 3 plates were 19, 13, and 13%, and the outlier rate was 13, 10, and 6%. The performance of the array was then tested in a different laboratory by examining the reproducibility of a single technical carcinoma across all 96 wells in a single plate (Table S5). Table S6 shows the calculated CVs for the single replicate. For each plate quarter (Q), the average CV for Q1 was 0.9969, for Q2 was 0.9968, for Q3 was 0.9972, and Q4 was 0.9954, with an overall average CV of 0.966.

Clinical Validity-"Fit for Purpose"

The performance of the assay was evaluated for its capability to classify tumors based on gene expression differences, and a secondary goal was to evaluate genes associated with biomarkers for potential therapies. Unsupervised hierarchical clustering was used to analyze log transformed normalized quantitative gene expression levels of 30 genes in 70 tumors. Clustering showed tumors segregated largely by histological type (Fig 1). For example, carcinomas segregated with E-cadherin (CDH1) expression, sarcomas segregated with vimentin (VIM) expression, and B-cell tumors segregated with CD79a. In addition, histologically similar tumors were separated into subtypes based on the expression of specific oncogenes such as mouse double minute 2 homologue (MDM2) and MET (Figs 1, 2). Gene expression was confirmed by IHC for tumor classifications by histogenesis for CDH1 and VIM, as well as highly expressed oncogenes MDM2 and MET (Fig 3).

Histologically related tumors were also interrogated for unique patterns in their gene expression. To further address the relationship between gene expression and protein expression in tumor subtypes, lymphomas were compared for MYC gene and protein expression. Figure 4 shows selected lymphomas with marked variation in MYC normalized mean gene expression values of 15,070 ± 770, 6,414 ± 22, and 2,960 ± 139, respectively, compared to IHC H-scores of 270, 260, and 120, respectively ($R^2 = 0.92$). B-cell (n = 9) and T-cell (n = 5) lymphomas were also compared for differences in gene expression (Fig 5). In addition to significant differences between CD4, CD79a, ITGAL, and ITGB2 in B- and T-cell lymphomas, E2F transcription factor 1 (E2F1), B-cell lymphoma 2 (BCL2), MAP2K1, and MAP2K2, but not MDM2, were significantly upregulated in T-cell compared to B-cell lymphomas ($P = .011$, .014, .011, and .047, respectively). In soft tissue sarcomas, E2F1, MDM2, MYC, and epidermal growth factor receptor (EGFR) varied

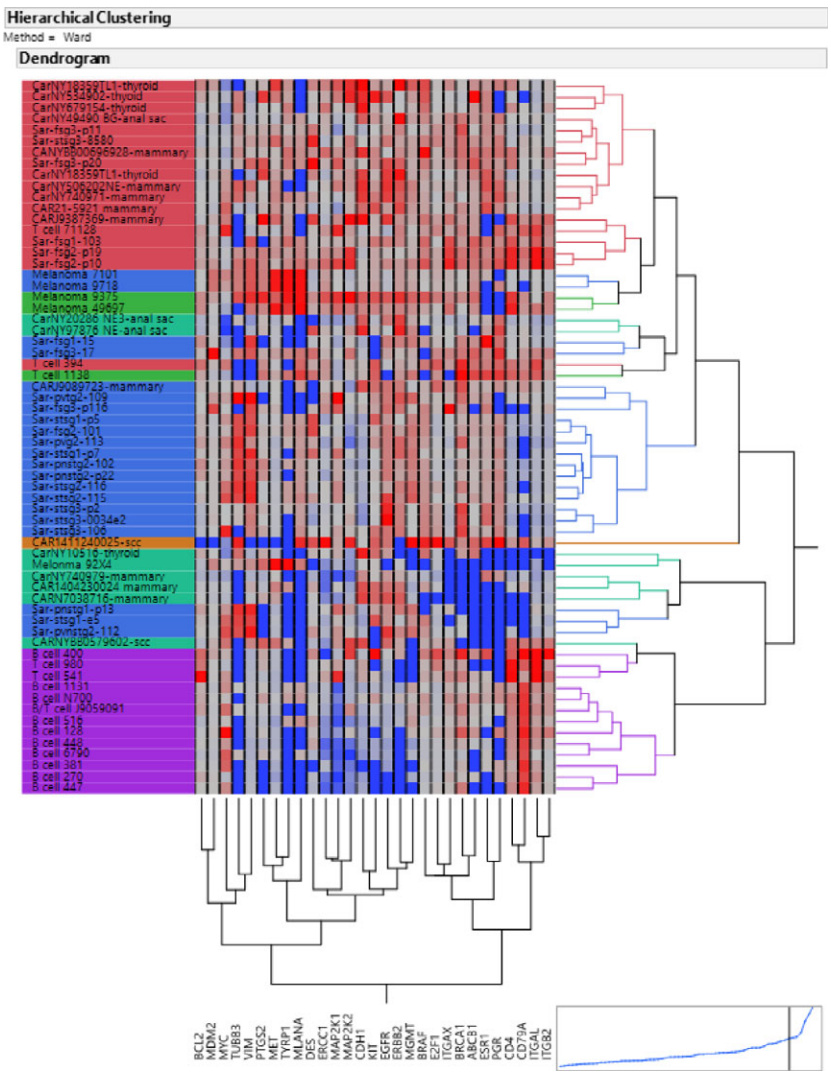

Fig 1. Unsupervised hierarchical classification of 70 canine tumors based on expression of 35 genes.

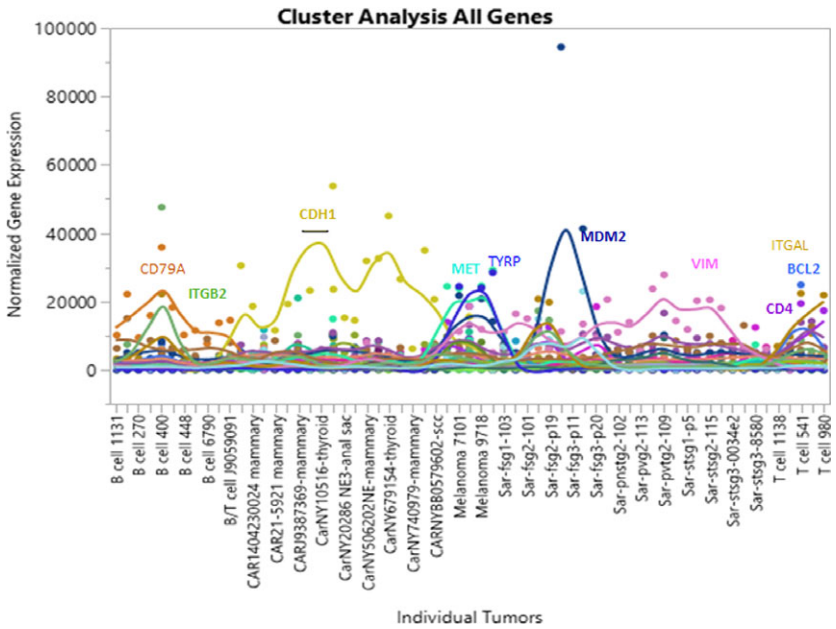

Fig 2. Smoothed line scatter plot of hierarchical clustering of canine tumors analyzed in Figure 1.

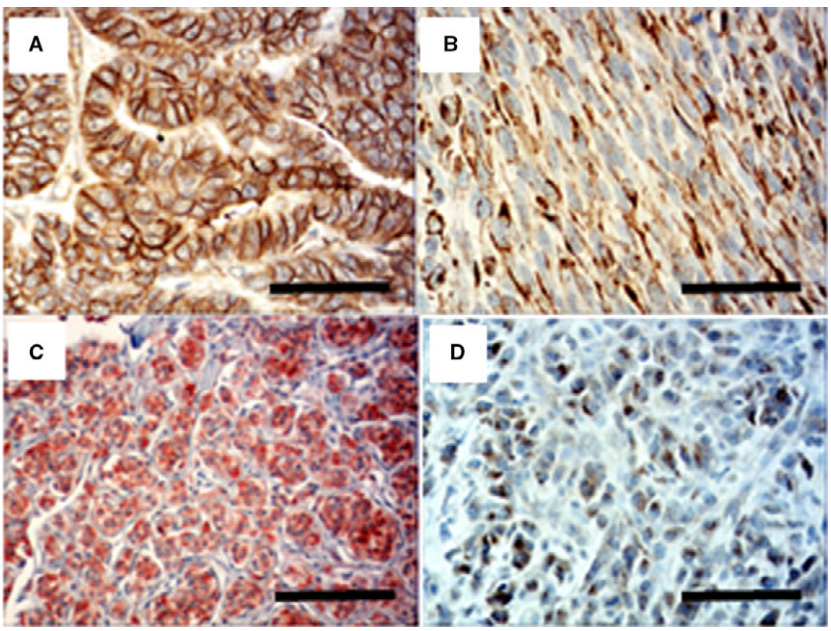

Fig 3. Photomicrographs of representative samples for immunohistochemistry of (**A**) E-cadherin in mammary carcinoma; (**B**) vimentin in a soft tissue sarcoma; (**C**) MDM2 in an amelanotic melanoma; (**D**) MET proto-oncogene receptor kinase (MET) in an amelanotic melanoma. Photomicrograph bar = 50 μm.

in expression levels (Fig 6), with E2F1 significantly upregulated in grade 3 (n = 8) compared to grade 2 (n = 10) and grade 1 (n = 6) (P = .0083). E2F1 was not upregulated in transitional cell carcinomas; however, prostaglandin synthase-2 (PTGS2) (COX-2) gene expression varied over 40-fold difference in gene expression (Fig 7A). IHC confirmed protein expression of COX-2 in this tumor compared to low expressing transitional cell carcinomas (TCC) with H-scores of 280 compared to 100, respectively (Fig 7B,C). Figure 8 compares expression of tyrosine kinase receptor levels in subsets of TCC, mammary adenocarcinomas, and melanomas showing both the variation between tumor types and variation within tumor types.

Discussion

Biomarkers provide unique clues about individual cancers, such as categorizing subtypes of tumors and

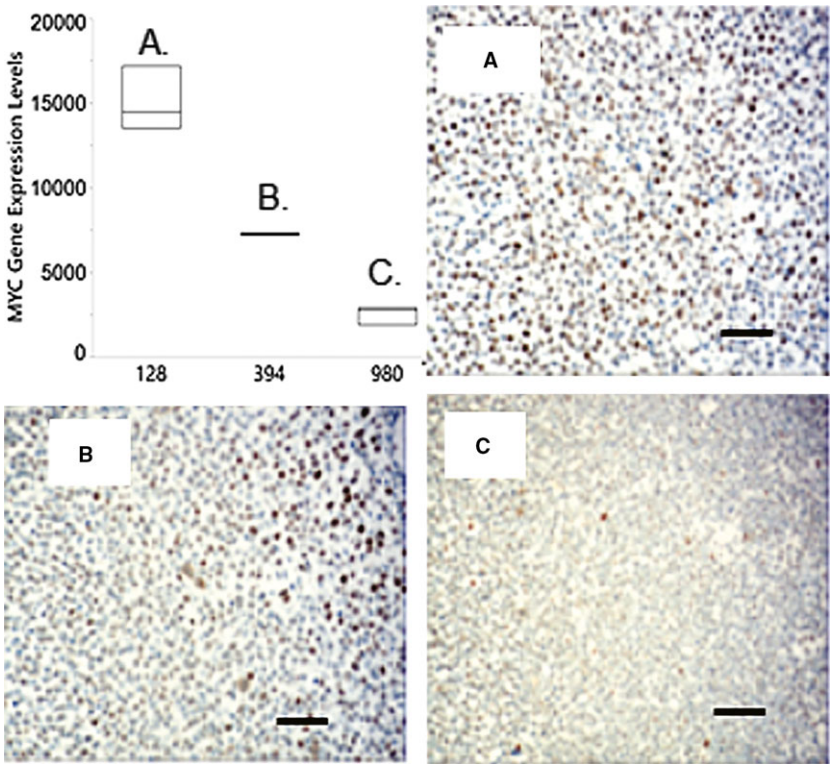

Fig 4. Comparison of MYC gene expression in 3 individual lymphomas (upper left pane) corresponding, respectively, to photomicrographs of MYC protein expression by immunohistochemistry Alphabetical letters A, B, and C designated in box plot correspond to A, B, and C labeled photomicrographs. Boxes in graph represent normalized mean expression ± SD from each individual tumor sample run in triplicate in the gene expression assay. Photomicrograph bar = 100 μm.

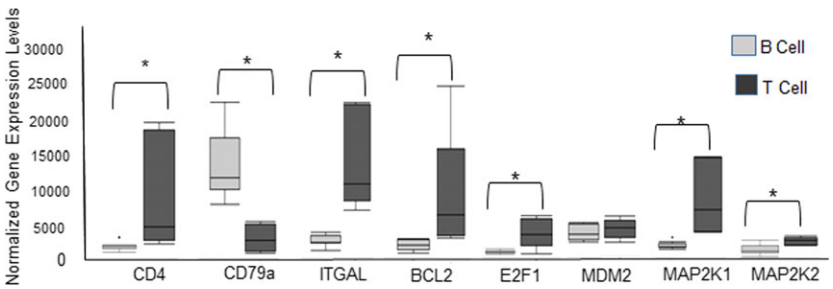

Fig 5. Comparison of gene expression levels in B-cell and T-cell lymphomas. Box plot represents normalized mean expression levels for individual B-cell lymphomas (n = 7) and T-cell lymphomas (n = 5) ± SD. *Significantly different at $P < .05$.

prognosticating which treatments are more likely to be effective or which therapies are more likely to fail. Combining molecular information with histopathology and clinical staging, individual treatment strategies can be designed for maximum effectiveness.[5,14] Indeed, gene expression studies are accepted in human oncology as a validated method to discover biomarkers of disease and determine treatment options for example in lymphoma,[15] breast,[16] bladder cancers,[17] sarcomas,[18] and other tumor types.[19] With the sequencing of the canine genome, similar biomarker strategies can be developed for veterinary diagnostics. Translating this knowledge, we detail a practical assay to profile the expression patterns of canine-specific genes in FFPE samples aiding diagnostic accuracy, and providing genomic information in support of deciding therapeutic options and potentially prognosis.

The impetus for developing the qNPA canine-specific assay described herein is to have an objective multi-analyte genomic test that can be successfully used in FFPE tissues and thereby incorporate into routine diagnostics and precision-based medicine. The automation of this assay allows for consistent results and rapid, 28-hour, turn-around time to provide a clinically relevant test. In the validation of this assay, we developed and tested oligo probe design and specificity and show the analytical precision, reliability, and reproducibility of the qNPA across array plates, instruments, and laboratories using common dog cancers obtained from clinical FFPE biopsy cases. As with other studies using qNPA

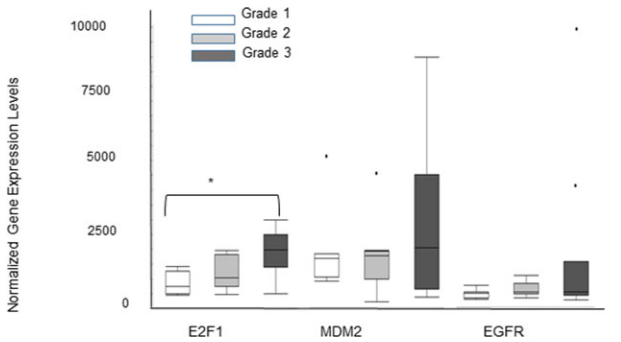

Fig 6. Comparison of gene expression levels in soft tissue sarcomas based on grade. Box plot represents normalized mean expression levels ± SD for individual grade 1 (n = 6), grade 2 (n = 10), and grade 3 (n = 8) soft tissue sarcomas. *Significantly different at $P < .05$.

approaches, we demonstrated that gene expression reflected semiquantitative protein expression by IHC across different tumor types and for a number of targets. In this regard, a qNPA-based assay has advantages to ancillary diagnostic tests such as IHC because qNPA quantitatively measures multiple biomarkers in small samples of FFPE biopsy tissues, while IHC is subjective or semiquantitative, relies on antibodies that may or may not be optimized for canine tumors, and has the limitation of 1 biomarker/slide. The multi-analyte gene expression capabilities in FFPE tissues also give qNPA advantages over RT-PCR for gene expression studies, which require significant optimization for FFPE samples.

Hierarchical clustering analysis showed that the genes on the assay discriminated tumors by histogenesis and therefore has use in support of diagnostically challenging cases, for example, amelanotic melanomas. Additionally, this analysis showed that tumors clustered by oncogene expression, with respect to or regardless of histogenesis. MET and other tyrosine kinase receptors such as EGFR and Erb-B2 receptor tyrosine kinase 2 (ERBB2) expression levels varied across sarcomas, carcinomas, and melanomas and additionally showed as much as 10-fold differences within the same tumor classifications. For example, MET expression was increased more than 8-fold in melanomas compared to carcinomas and sarcomas, but comparing individual melanomas, MET varied from no detectable expression to as much as a 20-fold upregulation when all genes were normalized to HK genes. Similarly, COX-2, a target of NSAIDS, was remarkably upregulated in one but not all TCC. Bladder cancers, also referred to as invasive urothelial cancer (iUC), are proposed as a relevant model for human iUC particularly due to the finding of EGFR and EGFR enriched gene expression in both.[20] Consistent with these finding, gene profiles in these samples identified upregulation of EGFR as well as ERBB2. Interestingly, MET and ERS1 expressions were also upregulated in bladder/urethral carcinomas in this study. In humans, both MET and ERS1 are overexpressed in aggressive bladder cancers and targeted

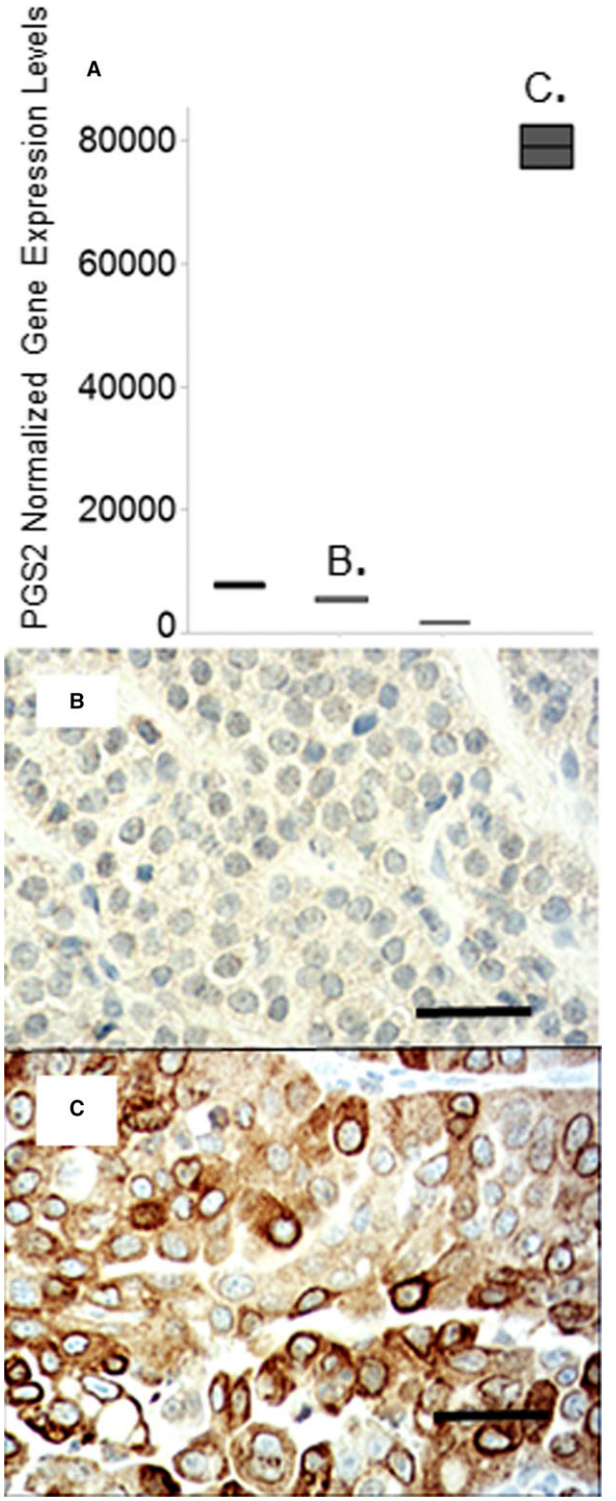

Fig 7. Comparison of COX-2 gene expression and PGS2 (COX-2) protein expression by immunohistochemistry (IHC) in transitional cell carcinomas (TCC). (**A**). The upper panel shows the normalized mean expression levels ± SD of PGS2 from individual tumor samples. The letters correspond to the images identified as (**B**) the photomicrograph of PGS2 IHC in TCC with an *H*-score of 290; and (**C**) PGS2 IHC in TCC with an *H*-score of 100. Photomicrograph bar = 50 μm.

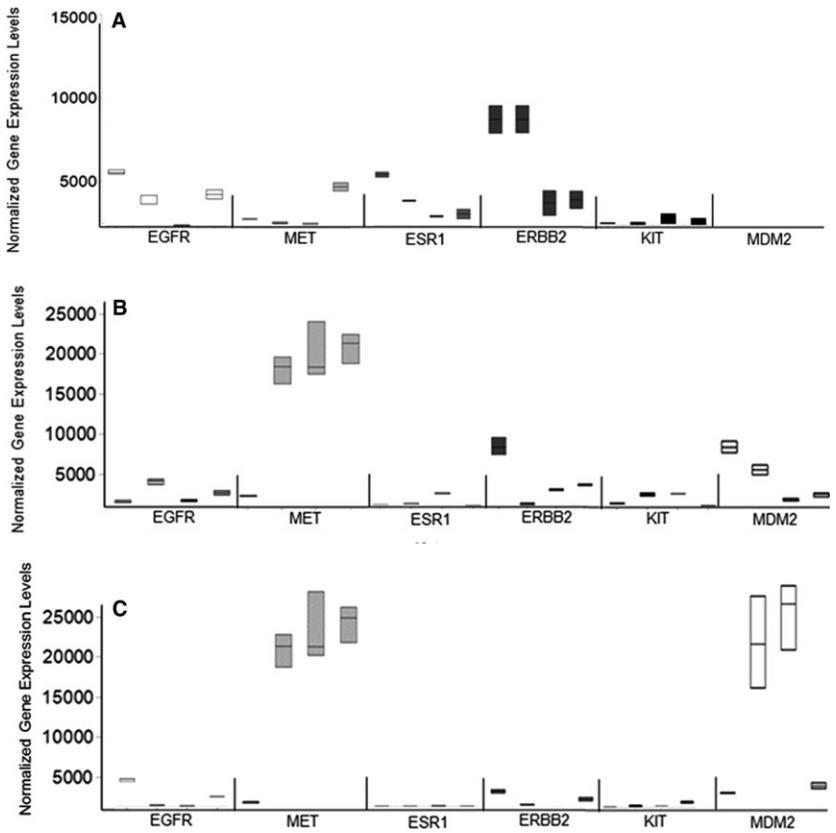

Fig 8. Comparison of expression of selected genes in representative tumors. (**A**) Normalized gene expression in TCC with bars representing mean ± SD of individual tumors run in triplicate in the quantitative nuclease protection assay; (**B**) normalized gene expression in mammary carcinomas with bars representing mean ± SD of individual mammary tumors run in triplicate; (**C**) normalized gene expression in melanomas with bars representing mean ± SD of individual tumors run in triplicate.

therapies aimed at these pathways are currently in clinical trials.[17,21] Such data show that dog cancers may be broadly categorized by histogenesis, but still have unique molecular fingerprints. It is with the understanding of the molecular fingerprints that therapies may be more precisely targeted.

We also observed gene signature patterns across tumor types that provide insights into the molecular mechanisms of canine cancers, particularly the expressions of MDM2 and E2F1. MDM2 was commonly upregulated across tumor types, and particularly melanomas, while E2F1 was significantly different between sarcoma grades and between B- and T-cell lymphomas. MDM2 and E2F1 upregulation and amplification are also commonly reported in melanomas, sarcomas, lymphomas, and some carcinomas in people.[22] Rezaie et al. reported MDM2 protein expression and limited polymorphisms in a small sample of canine tumors including mammary carcinoma and lymphoma,[23] and we observed protein expression in melanomas by IHC. MDM2 is the central regulator of p53 by mediating its ubiquitination and nuclear and cytoplasmic degradation.[24] Thus, by its action MDM2 suppresses p53 and overexpression of MDM2 is linked to an alternative pathway for wild-type p53-mediated oncogenesis. E2F1, a negative regulator of the tumor suppressor retinoblastoma gene, is linked to MDM2-p53 pathway in oncogenesis.[25] The function of these genes together represents fundamental mechanisms in the regulation of cancer and senescence resistance without mutations in p53. Using canine cancers to understand the role of these genes as well as testing therapies directed at these genes has the potential to greatly benefit both canine and human oncology.

Future studies will focus on defining and refining the clinical utility of FFPE-based gene expression assays and expanding their use in research and discovery. Clinical utility (distinguished from clinical validity) is achieved by showing that the test either improves outcome or the outcome is the same but derived at a lower cost.[12] Having the capability to use FFPE tumor biopsy samples certainly opens to the door to empower extensive clinical and translational studies.

Conclusion

Quantitative nuclease protection assay is a reliable robust gene expression assay with clinical validity to advance the use of molecularly based diagnostics in routinely collected FFPE samples from canine tumors.

Footnotes

[a] HTG Molecular Diagnostics, Inc., Tucson, AZ
[b] Declere, Cell Marque, Rocklin, CA
[c] Trilogy, Cell Marque, Rocklin, CA
[d] SAS Institute Inc., Cary, NC, 1989–2007

Acknowledgments

Conflict of Interest Declaration: The authors Davis, Barrett, Duchemin, and Post are founders and co-owners of the commercial company Innogenics that sponsored/funded the work presented in this manuscript. Post and Duchemin are also co-owners of the Veterinary Cancer Center, a privately owned veterinary cancer hospital. Dr. Schwartz is an employee of HTG Molecular, the commercial entity that holds patents and provides the platform equipment for the automated qNPA analysis. A number of steps were taken to avoid bias and conflict of interest. First, all samples that were analyzed in the studies were obtained retrospectively from independent histopathology laboratories with an accompanying diagnosis—Dr. Davis (DACVP) reviewed the slides for the assay to confirm samples and diagnosis, but not to change the diagnosis. When samples are analyzed in the assay, we have to have knowledge whether the sample is lymphoma, carcinoma, sarcoma or melanoma and its unique histopathology identifier (ie, slide number) to track the sample. However, the samples are quantified by the automated platform reported in an excel spreadsheet. Statistical analysis is performed on this data set. Immunohistochemistry was developed and performed at a separate histology laboratory using samples that had remaining slides available. *H*-scores were developed for the samples with knowledge of tumor type but not knowledge of results of the qNPA—that information was compared subsequently and statistical analysis applied. All authors reviewed, edited, and approved all versions of the manuscript.

Off-label Antimicrobial Declaration: Authors declare no off-label use of antimicrobials.

References

1. Albonico F, Mortarino M, Avallone G, et al. The expression ratio of miR-17-5p and miR-155 correlates with grading in canine splenic lymphoma. Vet Immunol Immunopathol 2013;155:117–123.

2. Frantz AM, Sarver AL, Ito D, et al. Molecular profiling reveals prognostically significant subtypes of canine lymphoma. Vet Pathol 2013;50:693–703.

3. Mudaliar MA, Haggart RD, Miele G, et al. Comparative gene expression profiling identifies common molecular signatures of NF-kappaB activation in canine and human diffuse large B cell lymphoma (DLBCL). PLoS ONE 2013;8:e72591.

4. Zamani-Ahmadmahmudi M, Najafi A, Nassiri SM. Reconstruction of canine diffuse large B-cell lymphoma gene regulatory network: Detection of functional modules and hub genes. J Comp Pathol 2015;152:119–130.

5. Klopfleisch R. Personalised medicine in veterinary oncology: One to cure just one. Vet J 2015;205:128–135.

6. Roberts RA, Sabalos CM, LeBlanc ML, et al. Quantitative nuclease protection assay in paraffin-embedded tissue replicates prognostic microarray gene expression in diffuse large-B-cell lymphoma. Lab Invest 2007;87:979–997.

7. Rimsza LM, Leblanc ML, Unger JM, et al. Gene expression predicts overall survival in paraffin-embedded tissues of diffuse large B-cell lymphoma treated with R-CHOP. Blood 2008;112:3425–3433.

8. Bourzac KM, Rounseville MP, Zarate X, et al. A high-density quantitative nuclease protection microarray platform for high throughput analysis of gene expression. J Biotechnol 2011;154:68–75.

9. Baker AF, Malm SW, Pandey R, et al. Evaluation of a hypoxia regulated gene panel in ovarian cancer. Cancer Microenviron 2015;8:45–56.

10. Rimsza LM, Wright G, Schwartz M, et al. Accurate classification of diffuse large B-cell lymphoma into germinal center and activated B-cell subtypes using a nuclease protection assay on formalin-fixed, paraffin-embedded tissues. Clin Cancer Res 2011;17:3727–3732.

11. Scott DW, Mottok A, Ennishi D, et al. Prognostic significance of diffuse large B-cell lymphoma cell of origin determined by digital gene expression in formalin-fixed paraffin-embedded tissue biopsies. J Clin Oncol 2015;33:2848–2856.

12. Henry NL, Hayes DF. Cancer biomarkers. Mol Oncol 2012;6:140–146.

13. Modur V, Hailman E, Barrett JC. Evidence-based laboratory medicine in oncology drug development: From biomarkers to diagnostics. Clin Chem 2013;59:102–109.

14. Heuckmann JM, Thomas RK. A new generation of cancer genome diagnostics for routine clinical use: Overcoming the roadblocks to personalized cancer medicine. Ann Oncol 2015;26:1830–1837.

15. Iqbal J, Naushad H, Bi C, et al. Genomic signatures in B-cell lymphoma: How can these improve precision in diagnosis and inform prognosis? Blood Rev 2016;30:73–88.

16. Rutter CE, Yao X, Mancini BR, et al. Influence of a 21-gene recurrence score assay on chemotherapy delivery in breast cancer. Clin Breast Cancer 2016;16:59–62.

17. Kim YW, Yun SJ, Jeong P, et al. The c-MET network as novel prognostic marker for predicting bladder cancer patients with an increased risk of developing aggressive disease. PLoS ONE 2015;10:e0134552.

18. Lesluyes T, Perot G, Largeau MR, et al. RNA sequencing validation of the Complexity INdex in SARComas prognostic signature. Eur J Cancer 2016;57:104–111.

19. Dietel M, Johrens K, Laffert MV, et al. A 2015 update on predictive molecular pathology and its role in targeted cancer therapy: A review focussing on clinical relevance. Cancer Gene Ther 2015;22:417–430.

20. Dhawan D, Paoloni M, Shukradas S, et al. Comparative gene expression analyses identify luminal and basal subtypes of canine invasive urothelial carcinoma that mimic patterns in human invasive bladder cancer. PLoS ONE 2015;10:e0136688.

21. Ghosh M, Brancato SJ, Agarwal PK, et al. Targeted therapies in urothelial carcinoma. Curr Opin Oncol 2014;26:305–320.

22. Burgess A, Chia KM, Haupt S, et al. Clinical overview of MDM2/X-targeted therapies. Front Oncol 2016;6:7.

23. Rezaie A, Tabandeh MR, Noori SM. Polymorphism of P53-Ets/AP1 transactivation region of MDM2 oncogene and its immunohistochemical analysis in canine tumours. Vet Comp Oncol 2016;14:137–146.

24. Mendoza M, Mandani G, Momand J. The MDM2 gene family. Biomol Concepts 2014;5:9–19.

25. Polager S, Ginsberg D. p53 and E2f: Partners in life and death. Nat Rev Cancer 2009;9:738–748.

Supporting Information

Additional Supporting Information may be found online in the supporting information tab for this article:

Fig S1. Schematic of qNPA Core Technology.

Fig S2. Assessment of oligonucleotide quality to ensure that each oligonucleotide functioned as intended.

Table S1. Accession numbers for genes selected for canine array.

Table S2. Housekeeping genes tested across different tumor types.

Table S3. Antibodies assessed for immunohistochemistry studies.

Table S4. Determining optimal tissue sample amount based on dilution linearity.

Table S5. Mean normalized values comparing gene expression levels from same mammary carcinoma applied in triplicate across all wells within the 96-well plate.

Table S6. Pearson's correlations for Table S5-single sample mammary carcinoma across all wells in 96 well plate.